Available online at www.sciencedirect.com
SCIENCE DIRECT®
Journal of Magnetic Resonance 166 (2004) 76–81
JMR Journal of Magnetic Resonance
www.elsevier.com/locate/jmr

Multi-echo imaging in highly inhomogeneous magnetic fields

F. Casanova, J. Perlo, B. Blümich,* and K. Kremer

Institut für Technieche und Macromolekulare Chemie, Aachen University of Technology, RWTH, D-52056 Aachen, Germany

Received 17 April 2003; revised 8 September 2003

Communicated by Joseph Ackerman

Abstract

A new pulsed field gradient multi-echo imaging technique to encode position in the phase of every echo generated by a CPMG sequence in the presence of a strongly inhomogeneous static magnetic field is presented. It was applied to improve the sensitivity in an imaging experiment by adding the echo train acquired during the CPMG sequence and to spatially resolve relaxation times of inhomogeneous specimens using single-sided probes. The sequence was implemented in a new bar-magnet MOUSE equipped with a gradient coil system to apply a pulsed magnetic field with a constant gradient along one spatial coordinate. An important reduction by a factor larger than two orders of magnitude in the acquisition time was obtained compared to the previously published single-point imaging technique.

Keywords: MRI; Unilateral NMR; Mobile probes; NMR-MOUSE

1. Introduction

Inside-out NMR uses single-sided sensors that define a sensitive volume inside the sample with a shape and a dimension determined by the size and geometry of the device [1–5]. With the open geometry of these sensors surface-near regions of objects unrestricted in size can be investigated via measurable relaxation times and diffusion coefficients. Potential applications include material analysis for quality control, porous media characterization in oil wells, safeguard of Cultural Heritage, and medical diagnostics.

Over the last few years and with the development of imaging methods for use in the presence of strongly inhomogeneous magnetic fields, the sample heterogeneity within the sensitive volume can be assessed with good spatial resolution. Not only an image which shows the density distribution can be produced but different NMR parameters like relaxation times and the local diffusion coefficient can also be spatially resolved in a non-destructive and non-invasive fashion.

Lateral space resolution has been previously achieved by implementing a single-echo pure phase-encoding imaging technique on sensors equipped with dedicated gradient coil systems [6,7]. The method combines a Hahn-echo sequence to refocus the magnetization spread due to the static gradient with the application of pulsed magnetic field gradients to encode position in the phase of the spin-echo signal. Using this single-point imaging method, 1D profiles with a spatial resolution of a few hundred microns were reported with measuring times of about 1 h.

Variant of the spin-echo technique can also be used to spatially resolve the relaxation time T_2 or the self-diffusion coefficient D along one- or two-space coordinates. The procedure demands the repetition of a set of imaging experiments with increasing echo-time in order to sample the local magnetization decay. The total time needed to obtain a relaxation/diffusion map is proportional to the number N_E of echo-time increments. This increase in the dimensionality of the spin-echo imaging experiment leads to extremely long acquisition times which limit the range of applications of this method.

To sample the complete echo decay in a single-imaging experiment CPMG-like sequences can be exploited for reduction of the acquisition time. This concept is known

* Corresponding author. Fax: +49-241-8022185.
E-mail address: bluemich@mc.rwth-achen.de (B. Blümich).

1090-7807/$ - see front matter © 2003 Elsevier Inc. All rights reserved.
doi:10.1016/j.jmr.2003.09.008

in the context of homogeneous static and rf magnetic fields [8,9]. But, the extension from a single- to a multi-echo imaging experiment in inhomogeneous magnetic fields is not straightforward. Due to off-resonance effects it is not possible to apply uniform plane rotations and the flip angle distribution inside each voxel introduces dramatic distortions in the phase encoding defined by the gradient pulses. In this work, we solved this problem by independent phase encoding of each echo of the CPMG sequence. Two gradient pulses with opposite polarities are applied between successive refocusing pulses, one before and one after the echo. The second gradient pulse completely cancels the phase spread introduced by the first one and leaves the magnetization before the next refocusing pulse with the original phase distribution of a conventional CPMG sequence. Either the echo signals can be added before image reconstruction to obtain a sensitivity enhancement or separated images can be reconstructed from each single-echo to obtain the complete relaxation decay for each pixel in a single-imaging experiment.

The new pulse sequence was successfully tested using a new bar-magnet NMR-MOUSE [5,7] equipped with a gradient coil array to produce a pulsed gradient along one spatial direction. The new multi-echo imaging sequence was applied to a silicon rubber sample with long T_2. The signal-to-noise ratio was improved by co-adding the echo train, and a complete 1D projection was obtained using a single scan. The method was also applied to spatially resolved the T_2 distribution of a heterogeneous object, demonstrating the possibility to locally measure the spin–spin relaxation time in a single-imaging experiment. As a last application a rapid acquisition with relaxation enhancement (RARE) sequence [9] was implemented to obtain T_2-weighted profiles in short time.

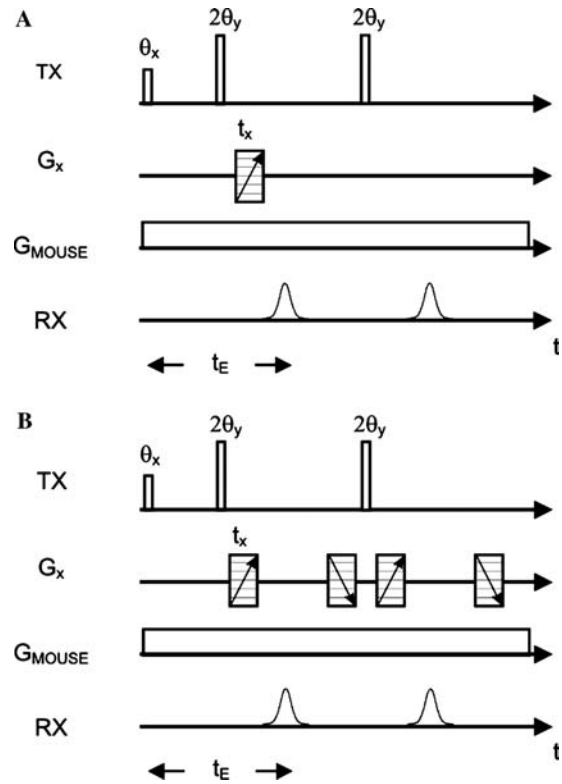

Fig. 1. Phase encoding multi-echo imaging with a CPMG pulse sequence. (A) Direct extension of the conventional single-point imaging method to a multi-echo version. The gradient pulse is applied after the first refocusing rf pulse. (B) To avoid phase distortions due to the loss of one component of the magnetization during the refocusing train, each echo is independently phase encoded in each interval. Before each echo a gradient pulse is applied to introduce a spatially dependent phase in the magnetization, and after sampling the maximum of the echo a second gradient pulse with opposite polarity is applied to cancel the phase distribution induced by the first gradient pulse.

2. Multi-echo imaging method

The direct extension from the single-echo technique to a multi-echo variant is the one shown in Fig. 1A, where a CPMG-like sequence is applied to repetitively refocus of the magnetization. In the presence of a slightly inhomogeneous static magnetic field $B_0(\omega_1 \gg \Delta\omega_0)$, and a homogeneous rf field B_1 to define a uniform plane rotation, the space encoding by the gradient pulses is the same for all the echoes; but in the presence of a strong static magnetic field gradient even a homogeneous rf field does not define a uniform plane rotation and the space encoding is not preserved when the refocusing pulses of the CPMG sequence are applied. The spin dynamics during the application of a CPMG-like sequence in the presence of grossly inhomogeneous B_0 and B_1 fields has been extensively analyzed by Hürlimann and Griffin [10] and by Balibanu et al. [11]. Hürliman and Griffin have demonstrated that for a standard CPMG sequence composed of a nominal $(\pi/2)_x$ pulse followed by a train of nominal $(\pi)_y$ pulses, the component along the y-axis of the magnetization tipped by the first rf pulse is preserved, while the x component goes to zero after a transient period. In this way the structure of the object, which can be obtained from the first echo, is progressive distorted with increasing echo number.

To analyze this problem the signal response was simulated assuming a static magnetic field along the z-axis with a constant gradient along the same direction, a homogeneous rf field perpendicular to the static magnetic field, and a pulsed magnetic field with a constant gradient along the x-axis. A homogeneous rf field was selected to show that the distortions are introduced by off-resonance effects. The evolution of the magnetization was calculated for non-interacting spins, taking into account the off-resonance effect during the rf pulses $(\omega_1 \sim \Delta\omega_0)$. The signal response of an object consisting of a single voxel positioned along the x-axis was calculated for the sequence of Fig. 1A using Eq. (1). The signal $S(n,k)$ is a complex matrix saving in the nth row the trace of k space sampled by the nth echo of the CPMG sequence. The resulting signal can be written as

$$S(n,k) = \int_{-\infty}^{\infty} \mathrm{d}\omega_0 \big[E_z(\omega_0, 2\tau - t_\mathrm{p}) \times P_{90}(\omega_0, 2\omega_1, t_\mathrm{p})\big]^n \times G_z(k) \times E_z(\omega_0, \tau - t_\mathrm{p}) \times P_0(\omega_0, \omega_1, t_\mathrm{p})\vec{M}_0, \quad (1)$$

where $P_0(\omega_0, \omega_1, pl)$ is the operator of a rf pulse of amplitude ω_1, length t_p and phase 0°. The effective rotation takes the off-resonance frequency ω_0 into account [12]; $E_z(\omega_0, t)$ is the operator of the free evolution period of duration t. It describes a rotation around the z-axis with an angle proportional to t and the off-resonance frequency ω_0; $G_z(k)$ is the operator of the gradient pulse. It describes a rotation around the z-axis with an angle determined by the amplitude of the stepped pulsed gradient, and by the position of the pixel along the gradient direction; and $\vec{M}_0$ is the thermal equilibrium magnetization.

Fig. 2A shows the spectra obtained from the phase modulation of each of the first eight simulated echoes. In agreement with the experimental results the 1D profile reconstructed from the phase modulation of the first echo (Hahn echo) is free of distortions. But with increasing echo number n a peak at the mirror frequency appears although the position of the pixel does not change. It is due to the distortion of one of the quadrature channels, which is completely attenuated after a few echoes. A second distortion is a contribution at the zero frequency, which originates in a stimulated echo, which is not modulated by the gradient pulse. This distortion is eliminated applying the gradient pulse before the first refocusing pulse. Fig. 2B shows the results obtained applying the pulsed gradient in the first free evolution period. Although the contribution at zero frequency is removed, the mirror spectrum, which reduces the field of view to only one quadrant, is still present. Fig. 2C shows the simulated profiles obtained using the pulse sequence proposed in this work (Fig. 1B). It can be observed that the phase distortion is completely eliminated, and the mirror peaks have disappeared from the profile. Also the contribution at zero frequency is removed as in the case of Fig. 2B.

The amplitude of each gradient pulse can be set equal in all the intervals sampling the same k space point for all the echoes of the train or it can be stepped to sample the complete k space in a convenient way during a CPMG train decay. When the same k space point is sampled in all the echoes a set of experiments must be repeated, increasing the amplitude of the gradient pulses step by step to cover the complete k space. The echoes sampled during the decay can be added to improve the signal-to-noise ratio obtaining a T_2-weighted profile, or the profiles reconstructed from each echo modulation can be plotted as a function of the echo time to measure the magnetization decay rate of each pixel. By changing the phase encoding scheme each echo during the train can be used to sample a different k-space point scanning the complete image in a single CPMG train. As small values of $|k|$ determine the contrast of the image, and the large ones determine the resolution, enhanced T_2 contrast can be obtained in a single CMPG experiment by sampling the $|k|$ values from maximum to zero [9].

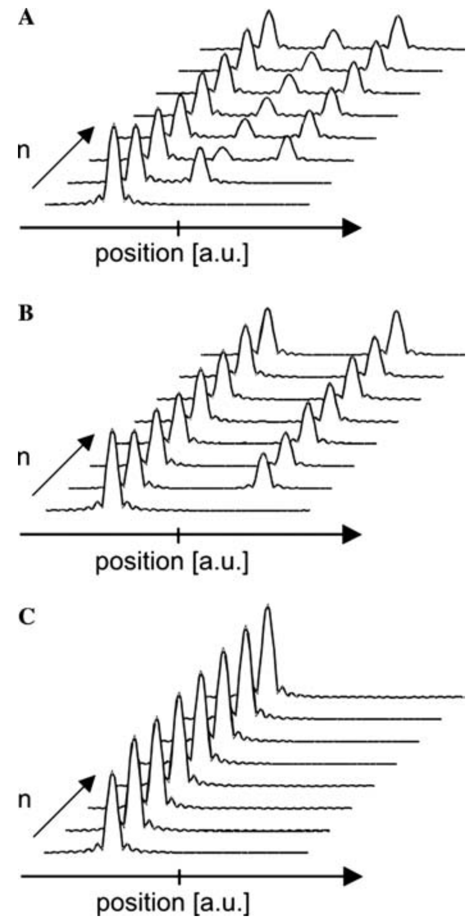

Fig. 2. Simulation of 1D profiles obtained as a function of the echo number for different encoding sequences. (A) Pulse sequence of Fig. 1A. Two different types of distortions are observed. The first is a signal contribution at zero frequency from the stimulated echo, and the second is a mirroring of the spectrum due to the loss of one component of the magnetization during the pulse sequence. (B) Pulse sequence of Fig. 1A, but pulsing the gradient in the first evolution period. Although the signal at zero frequency is removed the mirror spectrum is still present. (C) Pulse sequence of Fig. 1B. Both distortions are removed so that the complete echo train can be exploited to reduce the acquisition time.

To obtain the maximum number of echoes during the CPMG sequence a short echo time is desired, but it is limited by the rise and fall times of the gradient pulses. The phase defined by the gradient pulse applied before each echo must be completely cancelled by the gradient pulse applied following the echo. This condition determines that the echo time must be long enough to assure the second gradient pulse to be zero when the next rf pulse is applied. If this is not fulfilled a slightly different FoV is obtained from the even and the odd echoes, a fact that can be used to set a correct echo time. Depending on the T_2 values, use of a current pre-emphasis is needed to shape the current pulse, which drives the gradient coil.

3. Experimental setup

In this work a bar-magnet NMR-MOUSE [7] was used. It was furnished with a coil system to produce a pulsed field with a constant gradient. The NMR-MOUSE was constructed from a rectangular permanent magnet block with dimensions $45 \times 40 \times 20\,\text{mm}^3$, which provides a static magnetic field along the z-direction with a strong gradient of 16 T/m along the z-axis. The field variations along the x- and y-directions are smooth enough to define rather flat slices of constant frequency which is advantageous for slice selection along the z-axis by retuning the probe.

A figure-eight rf coil [7] positioned above the magnet pole face produced a B_1 field with a principal component perpendicular to B_0 in a region centered with the magnet. To produce pulsed gradients along the x-direction two 20 turn rectangular coils operating in series were mounted at opposite sides of the permanent magnet. The z component of the magnetic field produced by the coil pair posses a constant gradient in the region of interest suitable for space encoding. Using a Techron amplifier model 7541 to drive the coils, a gradient of about 0.24 T/m could be applied. To have the same spectral excitation bandwidth with both rf pulses (nominal $\pi/2$ and π pulses) their lengths were set equal, and their amplitudes were adjusted to maximize the echo amplitude.

4. Results

The new multi-echo technique was used to improve the signal-to-noise ratio in an imaging experiment adding all the echoes acquired in a CPMG sequence. The achievable reduction in measurement time that can be achieved by the multi-echo technique becomes really significant for samples with long T_2. To demonstrate this time saving an object from silicone rubber with $T_1 = 330\,\text{ms}$ and $T_2 = 70\,\text{ms}$ was constructed by arranging three rubber stripes 1.5 mm wide, 8 mm long, and 2 mm thick in parallel, separated by 1.5 mm, on the top of the rf sensor. The rf frequency was set to 14.8 MHz in order to select a slice at 1 mm depth. The sequence of Fig. 1B was applied using an echo time of $t_E = 0.2\,\text{ms}$ and gradient pulses 60 μs long. The gradient amplitude was increased in 32 steps sampling the k-space from negative to positive values. With the field of view set to 10 mm, a spatial resolution of about 0.3 mm was obtained. A single scan was used per gradient amplitude, improving the sensitivity by adding 250 echoes. A recycling delay of 1 s was used between experiments defining a total experimental time of 32 s needed to obtain a 1D profile. Fig. 3A shows the 1D

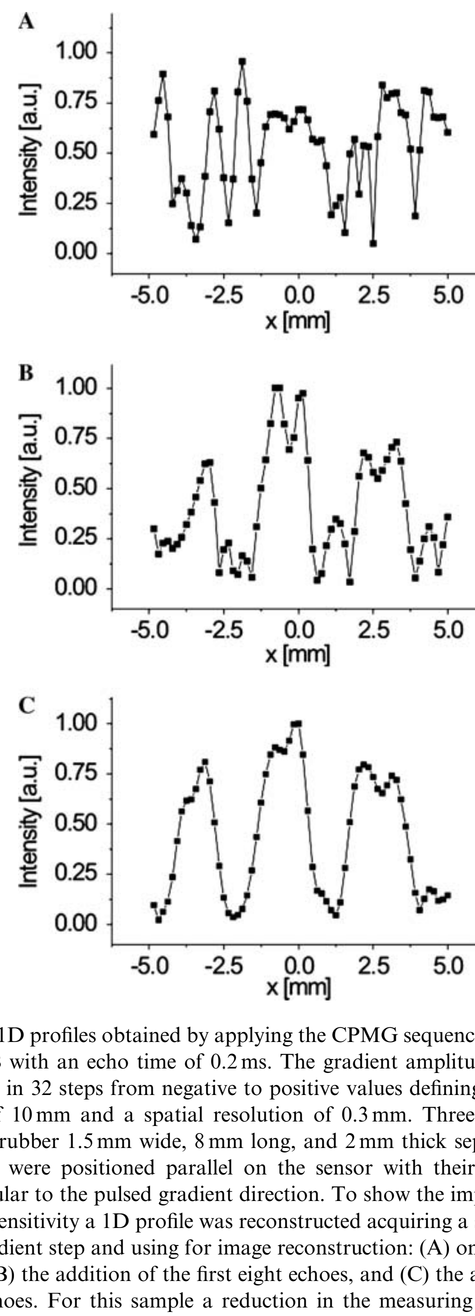

Fig. 3. 1D profiles obtained by applying the CPMG sequence shown in Fig. 1B with an echo time of 0.2 ms. The gradient amplitude was increased in 32 steps from negative to positive values defining a field of view of 10 mm and a spatial resolution of 0.3 mm. Three stripes of silicon rubber 1.5 mm wide, 8 mm long, and 2 mm thick separated by 1.5 mm were positioned parallel on the sensor with their axes perpendicular to the pulsed gradient direction. To show the improvement in the sensitivity a 1D profile was reconstructed acquiring a single scan per gradient step and using for image reconstruction: (A) only the first echo, (B) the addition of the first eight echoes, and (C) the addition of 250 echoes. For this sample a reduction in the measuring time by a factor of about 130 was achieved. Before adding the echo train for sensitivity improvement it was apodizated by its decay, which was previously measured.

projection obtained using only the first echo where only noise can be observed. Fig. 3B depicts the profile obtained by averaging the first eight echoes. Although noisy, the object structure can be observed. Finally, Fig. 3C shows the 1D projection obtained adding 250 echoes. The echo amplitude has decayed to half of its initial amplitude at the echo number 250, and approximating the decay of the intensity as exponential, this average is equivalent to the average of 130 Hahn echoes with full intensity. To obtain a 1D projection with the same signal-to-noise ratio applying a Hahn-echo sequence 130 scans are needed, and an experimental time of about 70 min would be required instead of the 32 s. This shows that an important time reduction can be obtained using the multi-echo acquisition method instead of the original single-echo technique.

As a second application a sample with a spatially varying T_2 was constructed from three stripes of different types of rubber using the same dimensions as in the previous experiment. The multi-echo sequence was applied with the same parameters as in the previous experiment, but 128 echoes were enough to correctly sample the longest decay present in the object. The repetition time was set three times the longest T_1 to avoid any T_1 weight in the image. Averaging 256 experiments a 1D profile was reconstructed from each echo. Fig. 4A shows the decay of the signal intensity spatially resolved along the x-axis as a function of the time. The different relaxation decays corresponding to each rubber stripe can be clearly distinguished. Fig. 4B shows the decay of three different pixels, one for each stripe. The decays were fitted using a biexponential function and the long relaxation time $T_{2,\mathrm{long}}$ of each rubber component is shown together with the fit.

As another application, and taking advantage of the independent space encoding that can be achieved in each echo, the RARE sequence was implemented to obtain

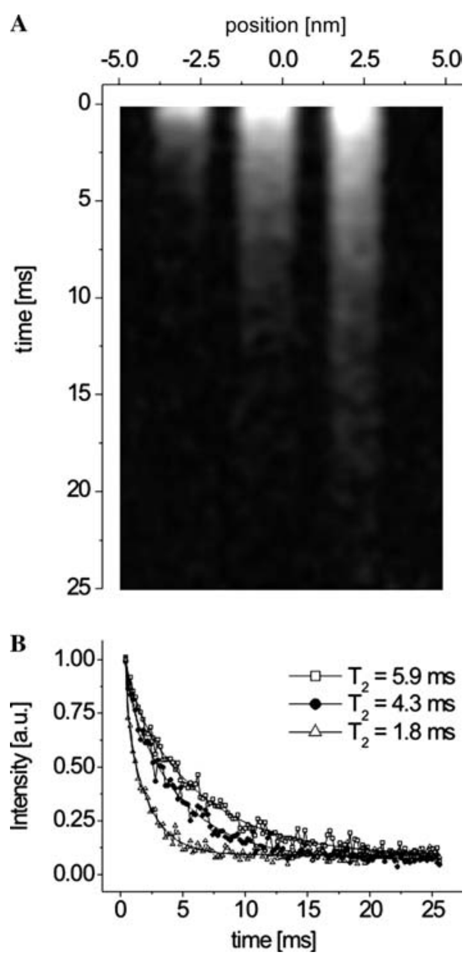

Fig. 4. Application of the sequence from Fig. 1B to obtain a T_2 parameter image. The sequence shown in Fig. 1B was applied using the same parameters as in the previous experiment. One hundred and twenty-eight echoes were acquired to correctly sample the longest decay present in the object using a repetition time, three times the longest T_1 of the sample. Two hundred and fifty-six scans were averaged for signal-to-noise improvement. (A) 1D profiles obtained from each echo plotted as a function of the echo time. The different relaxation times of the stripes can clearly be observed in the plot. (B) Intensity decay of one pixel selected from each stripe. The decays were fitted using a biexponetial function and the resultant $T_{2,\mathrm{long}}$ is given.

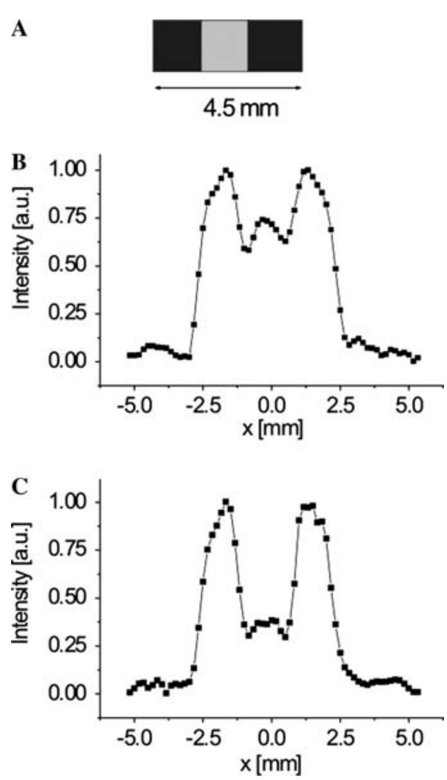

Fig. 5. Taking advantage of the independent phase encoding achieved in each echo, a RARE k space sampling was implemented to obtain a T_2-weighted 1D profile of the sample shown in (A). To compare the contrast, two different sampling patterns were used. The k space was sampled in an increasing way from zero to $k_{\max}$ (B), and in a decreasing way from $k_{\max}$ to zero (C). In experiment (B), a contrast of about 25% is obtained while using the proper RARE sequence a contrast of about 60% is achieved.

T_2-weighted profiles. For long enough T_2 values the complete 1D k space can be covered in a single experiment, consecutively sampling symmetric points of k space. Alternatively, to reduce the relaxation effect the k space can be sampled in two different experiments, the first sampling from maximum positive to zero and the second from maximum negative to zero, obtaining complete k space coverage by combining both experiments. Fig. 5 presents a comparison of the contrast obtained by sampling the k space in an increasing (B) and a decreasing way (C). For this comparison, a sample with three rubber stripes, two with a long T_2 and one with a short T_2, was built as shown in Fig. 5A. The stripes had the same dimensions as the ones used in the previous experiments. In case B, where small values of $|k|$ were acquired early in the echo train, the signal intensity of the center stripe is slightly different from that the others, showing a relative difference of only 25%. When small $|k|$ values were measured at the end in the CPMG train the intensity of the stripe is strongly affected leading to an enhancement in the T_2 contrast of more than 60%.

5. Conclusion

A pure phase encoding multi-echo imaging method to be used in the presence of a strongly inhomogeneous field was presented. The technique was applied to improve the signal-to-noise ratio corresponding to a reduction of the imaging time by up to two orders of magnitude. Alternatively, spatially resolved T_2 maps can be obtained in a single-imaging experiment. The features of this multi-echo acquisition scheme were demonstrated on phantoms made on rubber stripes showing different vulcanization degrees can be distinguished in the object. The new pulse sequence was implemented on a single-sided NMR sensor equipped with a gradient coil system to produce pulsed gradients along one spatial direction. It can be anticipated, that the new unilateral imaging sensor will find applications in non-destructive quality control and product failure analysis, where it can be used to inspect large objects from the surface. The extension of the 1D multi-echo sequence to a 2D version is straightforward as well as the implementation of the method to achieve 1D or 2D lateral resolution working in the stray field of superconducting magnets [13].

Acknowledgments

F.C. thanks the Alexander von Humboldt Foundation for the post-doctoral fellowship. Support of this project by the DFG Forschergruppe FOR333 Surface NMR of Elastomers and Biological Tissue is gratefully acknowledged.

References

[1] R.L. Kleinberg, A. Sezginer, D.D. Griffin, M. Fukuhara, Novel NMR apparatus for investigating an external sample, J. Magn. Reson. 97 (1992) 466–485.
[2] G.A. Matzkanin, A review of non-destructive characterization of composites using NMR, in: Nondestructive Characterization of Materials, Springer, Berlin, 1998, p. 655.
[3] R.L. Kleinberg, Well logging, in: D.M. Grant, R.K. Harris (Eds.), Encyclopedia of NMR, Wiley, New York, 1996, pp. 4960–4969.
[4] G. Eidmann, R. Salvelsberg, P. Blümler, B. Blümich, The NMR-MOUSE, a mobile universal surface explorer, J. Magn. Reson. A 122 (1996) 104–109.
[5] B. Blümich, V. Anferov, S. Anferova, M. Klein, R. Fechete, M. Adams, F. Casanova, A simple NMR-MOUSE with a bar magnet, Magn. Reson. Eng. 15 (4) (2002) 255–261.
[6] P. Prado, B. Blümich, U. Schmitz, One-dimensional imaging with a palm-size probe, J. Magn. Reson. 144 (2000) 200–206.
[7] F. Casanova, B. Blümich, Two-dimensional imaging with a single-sided NMR probe, J. Magn. Reson. 163 (2002) 38–45.
[8] P.T. Callaghan, Principle of Nuclear Magnetic Resonance Microscopy, Clarendon Press, Oxford, 1991.
[9] B. Blümich, NMR Imaging of Materials, Oxford University Press, Oxford, 2000.
[10] M.D. Hürlimann, D.D. Griffin, Spin dynamics of Carr-Purcel-Meibohm-Gill-like sequences in grossly inhomogeneous B_0 and B_1 fields and applications to NMR well logging, J. Magn. Reson. 143 (2000) 120–135.
[11] F. Balibanu, K. Hailu, R. Eymael, D. Demco, B. Blümich, Nuclear magnetic resonance in inhomogeneous magnetic fields, J. Magn. Reson. 145 (2000) 246–258.
[12] R.R. Ernst, G. Bodenhausen, A. Wokaun, Principles of Nuclear Magnetic Resonance in One and Two Dimensions, Clarendon Press, Oxford, 1987.
[13] J. Godward, E. Ciampi, M. Cifelli, P.J. McDonald, Multidimensional imaging using stray field pulsed gradients, J. Magn. Reson. 155 (2002) 92–99.